Accurate determination of the anisotropy factors and the phase differences of Raman polarizabilities in some uniaxial crystals: the case of lithium niobate

2009 J. Phys.: Condens. Matter 21 015905

(http://iopscience.iop.org/0953-8984/21/1/015905)

J. Phys.: Condens. Matter **21** (2009) 015905 (9pp) doi:10.1088/0953-8984/21/1/015905

Accurate determination of the anisotropy factors and the phase differences of Raman polarizabilities in some uniaxial crystals: the case of lithium niobate

N Djiedeu[1], B Mohamadou[1], P Bourson[2] and M Aillerie[2]

[1] Centre for Atomic Molecular Physics and Quantum Optics (CEPAMOQ), University of Douala, Cameroon
[2] Laboratoire Matériaux Optiques, Photonique et Systèmes, UMR CNRS 7132, Université Paul Verlaine–Metz et Supelec, 2 rue E. Belin, F-57070 Metz, France

E-mail: djienico@yahoo.fr, ballo_mohamadou@yahoo.fr, bourson@metz.supelec.fr and aillerie@metz.supelec.fr

Received 22 October 2008, in final form 30 October 2008
Published 1 December 2008
Online at stacks.iop.org/JPhysCM/21/015905

Abstract
The present study highlights self-consistently helpful improvements dedicated to overcoming the difficulty resulting from the fitting procedure of integrated Raman intensities recorded according to the rotation crystal method described earlier. To this end, the anisotropy factors of Raman polarizabilities and the corresponding relative phases are determined within the framework of the exact mathematical derivation of the phase factors. These are the relevant parameters of the Raman efficiency relations which are numerically difficult to obtain from the fitting of the integrated areas. The present theoretical approach is then applied to the modes of the A_1 and Ey symmetry species of the lithium niobate (LN) crystal point group. All the expressions of the Raman absolute intensities of the A_1 and Ey irreducible representations initially imply three parameters to be determined from the fitting computations. However, from the derived analytical expressions of the phase differences, the number of parameters involved in the fitting procedure is reduced from 3 to 2, thus improving the statistics of the numerical treatment.

1. Introduction

In the connection between the electro-optic coefficients and Raman scattering, the highest source of error is related to the absolute or relative determination of Raman polarizabilities. Direct measurements are less accurate because of the variability of the steps in the spectral acquisition chain, for example the apparatus function of the spectrometer, the detector spectral sensitivity, as well as the noise equivalent power. Relative measurements are preferred even if they need a standard. For most of the measurements one always needs to fit the response functions to evaluate the Raman polarizabilities. Mooradian [1] and McWhorter have used the response functions of plasmons and LO phonons in GaAs to determine Raman polarizabilities as well as the corresponding second harmonic generation coefficients. Loa *et al* [2] measured indirectly the tensor elements of the Raman scattering in thin sample films of GaN by measurement of the Raman efficiencies at different distances from the laser focus. Nippus [3] has used the simplified Raman profile to determine peak areas and relative Raman tensor that he then converted to the relative Raman tensor polarizabilities. Strach *et al* [4] have used both rotations of the polarizers and the analysers to obtain the Raman intensities. Moreover, they used arbitrary data to adjust these Raman intensities. More recently, Djiedeu *et al* [5], by rotating the crystal in steps of 10°, have demonstrated a general method for the determination of the Raman efficiencies in the backscattering configuration for parallel and perpendicular polarizers. The method of crystal rotation allows us to express the Raman efficiencies of C_{3v} crystals as a function of crystal rotation angle. In previous studies [4, 5] such expressions of the Raman

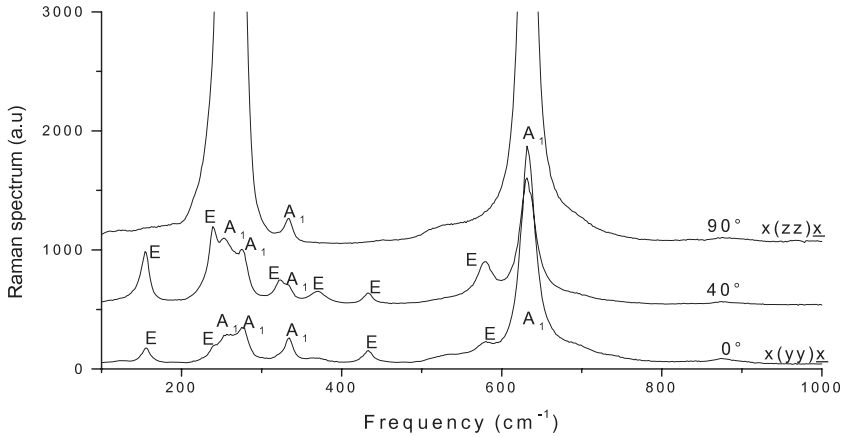

Figure 1. Raman spectra of a pure $LiNbO_3$.

efficiencies were directly used to fit experimental curves. Therefore it was very difficult to determine some parameters like phase differences, anisotropy factors and extrema positions of the Raman efficiency. In this study we propose a new approach allowing unambiguously the determination of these parameters. This paper is organized into five sections. Section 2 is an indication of the measurement procedure of the Raman spectra and the presentation of experimental results prior to their analysis. In section 3 we present the analytical treatment of the Raman spectra based on a rigorous mathematical approach. We have calculated some theoretical parameters of C_{3v} crystals for both A_1 and Ey modes, for example the phase difference, for which we have demonstrated its uniqueness. Section 4 presents the application of this study to the lithium niobate crystal and the experimental results. Finally, we compare our work with previous studies, discuss the results and conclude about the accuracy and the generalization of our method.

2. Procedure of the Raman spectra measurement

The experimental set-up and the studied crystal have been described in [5]. The stoichiometric lithium niobate crystal belongs to the C_{3v} point group whose associated Raman tensors with active modes are [6]

$$A_1(z) = \begin{pmatrix} a & 0 & 0 \\ 0 & a & 0 \\ 0 & 0 & b \end{pmatrix}, \qquad E(x) = \begin{pmatrix} 0 & c & d \\ c & 0 & 0 \\ d & 0 & 0 \end{pmatrix}, \qquad E(y) = \begin{pmatrix} c & 0 & 0 \\ 0 & -c & d \\ 0 & d & 0 \end{pmatrix}. \tag{1}$$

The letters in parentheses indicate the direction of the polarization associated with the modes with respect to the crystallographic axis. In order to simplify the notation, we set $E(x) = Ex$ and $E(y) = Ey$. The complex numbers a, b, c and d are the Raman tensor components which can be selected by the polarization filter (ij) (i, j being the dielectric axes of the crystal which are assumed to be identical to the laboratory axes; the polarization filter is equivalent to the basis functions of the C_{3v} point group). The Raman spectra were recorded using the backscattering scheme $x(yy)\underline{x}$ ($\theta = 0°$) to $x(zz)x$ ($\theta = 90°$) in steps of 10°. θ is the crystal rotation angle around the x dielectric axis. According to (1), both the A_1 (TO) and Ey(TO) Raman modes will be activated in the same spectrum (figure 1). At $\theta = 40°$, the structures belonging to the Ey symmetry species present an intensity enhancement while these lines totally disappear at $\theta = 90°$ corresponding to the polarization filter (zz). As a consequence, rotating the crystal preserves the selection rules worked out from group theoretical considerations.

3. Analytical treatment of the Raman spectra

3.1. Intensity of a Raman line

According to the fluctuation–dissipation theorem [7], the Raman intensity of a symmetric Raman line and for a transverse optical mode is described by a Lorentz profile as

$$\frac{\mathrm{d}^2 I}{l\,\mathrm{d}\omega\,\mathrm{d}\Omega} \propto A_0 . \frac{\Gamma\omega\omega_0^2}{(\omega^2-\omega_0^2)^2+\Gamma^2\omega^2}(n(\omega)+1) \tag{2}$$

where I is the intensity of the Raman line,

A_0: amplitude of the Lorentz profile, ω_0: frequency of the TO phonon,

Γ: damping parameter of the phonon mode, l: scattering length in the crystal,

$n(\omega)$: thermal population factor, Ω: solid angle.

We have used equation (2) for the fitting of the parameters (A_0, ω_0, Γ) of all the peaks. These parameters will be used to evaluate the peak areas of the Raman line.

3.2. Area fitting

Using the approximation $\omega \sim \omega_0$, equation (2) can be rewritten as

$$\frac{\mathrm{d}^2 I}{l\,\mathrm{d}\omega\,\mathrm{d}\Omega} \propto S(\omega) = S_{\max}\frac{(\Gamma/2)^2}{(\omega-\omega_0)^2+(\Gamma/2)^2} \tag{3}$$

where

$$S_{\max} = A_0\frac{\omega_0}{\Gamma}(n(\omega_0)+1) \tag{4}$$

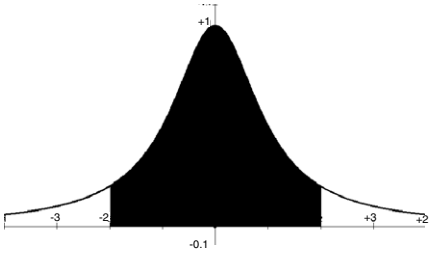

Figure 2. Peak area of a Raman line.

$S(\omega)$: amplitude of the Raman line for a given ω, $S_{\max}$: maximum amplitude of the Raman line [3].

It can be shown easily using equation (3) that Γ is the full width at half-maximum. This is due to the approximation $\omega \sim \omega_0$. Nippus [3] has used a simplified Lorentz profile to evaluate the parameters ($S_{\max}$, ω_0, Γ) and the peak areas. Therefore, with the aim of comparing our results with those of Nippus, we have used equation (3) to evaluate the peak areas. We obtained

$$\frac{\mathrm{d}I}{\mathrm{d}\Omega} \propto S = \frac{1}{\Gamma}\int_{\omega_0-\Gamma}^{\omega_0+\Gamma} S(\omega)\,\mathrm{d}\omega = S_{\max}\arctan(2) \qquad (5)$$

where S is the peak area of the Raman profile. S and $S_{\max}$ are dimensionless quantities. Equation (5) shows that the Raman line intensity can be considered proportional to the integrated area. The integrated areas proportional to the Raman intensities of the transverse modes of A_1 and Ey modes are evaluated over an interval 2Γ as shown in figure 2. This is to avoid errors due to the base line asymmetry and to take into account the approximation $\omega \sim \omega_0$. The use of equation (5) then improves the calculation of peak areas rather than the approximation of the isosceles triangle used previously [5].

3.3. Raman intensities

The absolute Raman intensity can be calculated [4] using the relation

$$I = |e_s^* P e_i|^2 \qquad (6)$$

where P is the Raman tensor of the uniaxial crystals given in equations (1),

e_i: polar unit vector of the incident polarization,

e_s^*: polar and transposed matrix of the scattered polarization unit vector.

For the backscattering geometrical configuration $x(\cdots)\underline{x}$, these unit vectors are contained in the (yz) plane. We have derived the Raman intensity expressions for C_{3v} crystals using equations (1) and (6) for A_1 and Ey modes. It then follows that

$$I_{yz}^{A_1(\theta)} = (1/2)(|a|^2 + |b|^2 - 2|a||b|\cos\varphi_{ba})\sin^2(2\theta) \qquad (7)$$

$$I_{yy}^{A_1(\theta)} = |a|^2\cos^4\theta + |b|^2\sin^4\theta + (1/2)|a||b|\sin^2(2\theta)\cos(\varphi_{ba}) \qquad (8)$$

$$I_{zz}^{A_1(\theta)} = |a|^2\sin^4\theta + |b|^2\cos^4\theta + (1/2)|a||b|\sin^2(2\theta)\cos\varphi_{ba} \qquad (9)$$

$$I_{yz}^{Ey(\theta)} = (1/4)|c|^2\sin^2(2\theta) + |d|^2\cos^2(2\theta) - (1/2)|c||d|\sin(4\theta)\cos(\varphi_{dc}) \qquad (10)$$

$$I_{yy}^{Ey(\theta)} = |c|^2\cos^4\theta + |d|^2\sin^2(2\theta) + 2|c||d|\cos^2(\theta)\sin(2\theta)\cos(\varphi_{dc}) \qquad (11)$$

$$I_{zz}^{Ey(\theta)} = |c|^2\sin^4(\theta) + |d|^2\sin^2(2\theta) - 2|c||d|\sin^2(\theta)\sin(2\theta)\cos(\varphi_{dc}) \qquad (12)$$

$|a|, |b|$ are the absolute tensor elements of the Raman scattering of the A_1 symmetric modes. $|c|, |d|$ are the absolute tensor elements of the Raman scattering of the Ey symmetric modes, while φ_{ba} and φ_{cd} are the phase differences, respectively, for the A_1 and Ey modes, and θ is the angle of the crystal rotation. We have to notice that a θ rotation of the crystal corresponds to a $-\theta$ rotation of the polarization unit vectors. Diagonal elements are obtained for parallel polarizations ($e_i \parallel e_s$) and nondiagonal elements are obtained for crossed polarizations ($e_i \perp e_s$). For example, equation (7) has been obtained using $e_i(0, \cos\theta, -\sin\theta)$ and $e_s^*(0, \sin\theta, \cos\theta)$. Equations (7) and (9) have been derived previously by Strach [4] with another approach. In equations (7)–(12), the subscripts ij of the Raman intensities are the initial state of the polarization filter while the superscripts refer to the polar irreducible representation of the C_{3v} crystal point group. Since the Raman spectra are recorded by stepping the rotation of the crystal for each ten degrees, relation (7)–(12) can be used for the experimental data determined in the framework of the response function.

Each of these Raman intensities contains three unknown parameters, which are two Raman tensor elements or Raman polarizabilities and their phase difference. A fit with three parameters is a source of large errors. Knowing that the phase differences are functions of the absolute Raman polarizabilities, it is possible to reduce these three parameters to two by differentiating the Raman intensities and separating the variables. Details of the change of variables and use of the anisotropy parameters are given in the appendix.

3.4. Anisotropy parameters

We have used these parameters to rewrite the Raman efficiencies defined in equations (7)–(12) in a useful form. We will see later that the anisotropy parameters are very important for the direct determination of the anisotropy factors and the phase differences.

For the A_1 mode, we have defined the anisotropy parameter β by

$$\cos\beta = \frac{|a|}{\sqrt{|a|^2+|b|^2}}, \qquad \sin\beta = \frac{|b|}{\sqrt{|a|^2+|b|^2}}. \qquad (13)$$

For the Ey mode, we have defined the anisotropy parameter α by

$$\cos\alpha = \frac{|c|}{\sqrt{|c|^2+4|d|^2}}, \qquad \sin\alpha = \frac{2|d|}{\sqrt{|c|^2+4|d|^2}}. \qquad (14)$$

The anisotropy parameters are derived experimentally during the fitting procedure.

Using these expressions and differentiating the Raman efficiencies, we have obtained the derived equations as functions of the phase difference and the extrema positions. We have separated these variables and obtained, on the one hand, the phase differences of Raman polarizabilities and, on the other hand, the extrema positions of the Raman efficiencies.

3.5. Theoretical results for the A1 mode

3.5.1. Anisotropy factor. In the literature [4] the anisotropy factors are sometime defined as the ratio between Raman polarizabilities. This is the definition we have used in this work. Using equation (13), we obtain the anisotropy factor given by

$$\frac{|b|}{|a|} = \tan\beta. \tag{15}$$

3.5.2. Phase differences. The phase differences are given by

$$\varphi_{ba} = \pm 2\beta \qquad \text{or} \qquad \varphi_{ba} = \pm(\pi \pm 2\beta). \tag{16}$$

The sign + or − takes into account the fact that b is damped with respect to a or conversely.

We can choose the phase difference to be positive.

3.5.3. Extrema positions of the Raman efficiencies. During the fitting procedure, we should be able to check the number of extrema expected. The extrema are

$$\cos(2\theta_0) = \frac{\cos(2\beta)}{-1+\sin(2\beta)\cos(2\beta)} \qquad \text{or}$$
$$\cos(2\theta_0) = \frac{\cos(2\beta)}{-1-\sin(2\beta)\cos(2\beta)} \tag{17}$$

$$\theta = \frac{2k\pi}{2}, \qquad \theta = \frac{\pi}{2} + \frac{2k\pi}{2}, \qquad k \in \{0, 1\}. \tag{18}$$

3.6. Theoretical results for the Ey mode

By analogy with the A_1 mode, we have obtained the following results for the Ey mode.

3.6.1. Anisotropy factors. The anisotropy factor is defined by the equation below:

$$\frac{|d|}{|c|} = \frac{1}{2}\tan\alpha. \tag{19}$$

3.6.2. Phase differences. The phase differences are given by

$$\varphi_{\mathrm{dc}} = \pm 2\alpha \qquad \text{or} \qquad \varphi_{\mathrm{dc}} = \pm(\pi \pm 2\alpha). \tag{20}$$

3.6.3. Extrema positions. The extrema positions are given by

$$\theta_0 = \frac{k\pi}{4} + \arctan(\sin(2\alpha)) \qquad \text{or}$$
$$\theta_0 = \frac{k\pi}{4} + \arctan(-\sin(2\alpha)), \qquad k \in \{0, 1, 2, 3\}. \tag{21}$$

3.7. Fitting of the Raman intensities

The above parameters allow us to reduce the number of fitting parameters from 3 to 2 and to express the Raman efficiency as functions of only two parameters. Then, using the relation of proportionality (5) between the integrated area and the Raman intensity, we have been able to express the integrated areas as functions of the anisotropy parameters and the crystal rotation angle:

$$S_{yz}^{A_1(\theta)} = (a_0)^2(1+(\tan\beta)^2)(1 \mp \sin(4\beta))\sin^2(2\theta) \tag{22}$$

$$S_{yy}^{A_1(\theta)} = (a_0)^2(1+(\tan\beta)^2)[\cos^2\beta\cos^4\theta + \sin^2\beta\sin^4\theta \pm (1/8)\sin(4\beta)\sin^2(2\theta)] \tag{23}$$

$$S_{zz}^{A_1(\theta)} = (a_0)^2(1+(\tan\beta)^2)[\cos^2\beta\sin^4\theta + \sin^2\beta\cos^4\theta \pm (1/8)\sin(4\beta)\sin^2(2\theta)] \tag{24}$$

$$S_{yz}^{Ey(\theta)} = (1/8)(c_0)^2(1+\tan^2\alpha)[1-\cos(2\alpha) \times \cos(4\theta) \pm (1/2)\sin(4\alpha)\sin(4\theta)] \tag{25}$$

$$S_{yy}^{Ey(\theta)} = (1/2)(c_0)^2(1+\tan^2\alpha)[1+\cos(2\alpha) \times \cos(2\theta) \mp (1/2)\sin(4\alpha)\sin(2\theta)]\cos^2(\theta) \tag{26}$$

$$S_{zz}^{Ey(\theta)} = (1/2)(c_0)^2(1+\tan^2\alpha)[1-\cos(2\alpha) \times \cos(2\theta) \pm (1/2)\sin(4\alpha)\sin(2\theta)]\sin^2(\theta) \tag{27}$$

where

$$a_0 = \delta_0|a| \qquad \text{and} \qquad c_0 = \eta_0|c| \tag{28}$$

a_0 and c_0 are defined as lengths and are derived from fits to the experimental data. δ_0 and η_0 are the square roots of the coefficients of proportionality between the integrated area and the Raman intensity for A_1 and Ey modes, respectively. The sign + or − is directly related to the phase difference used. These functions have a periodicity of π or $\pi/2$.

We can see that the peak areas are expressed as functions of only two parameters. This is a major advantage because of the accuracy of the results provided and the time saved during the fitting procedures. The optimal parameters are those allowing the best fitting of the experimental curves.

3.8. Uniqueness of the phase difference

The Raman intensities (11) and (12) are nonlinear and symmetric functions. We have studied equation (11) in order to check the uniqueness of the phase difference. We assume first of all that we do not know the expression of the phase difference. After studying the Raman efficiency in the case of parallel polarizers for the Ey mode, we have shown that there exists no other solution.

3.8.1. Derivative equations. The derivative of the Raman efficiency (11) leads to two equations:

$$\cos\theta = 0 \tag{29}$$

$$\tan^3\theta + 3\frac{\cos\varphi_{\mathrm{dc}}}{\tan\alpha}\tan^2\theta + \left(\frac{2}{\tan^2\alpha} - 1\right)\tan\theta - \frac{\cos\varphi_{\mathrm{dc}}}{\tan\alpha} = 0. \tag{30}$$

The first has a trivial solution which is $\pi/2$ and the second is a polynomial equation.

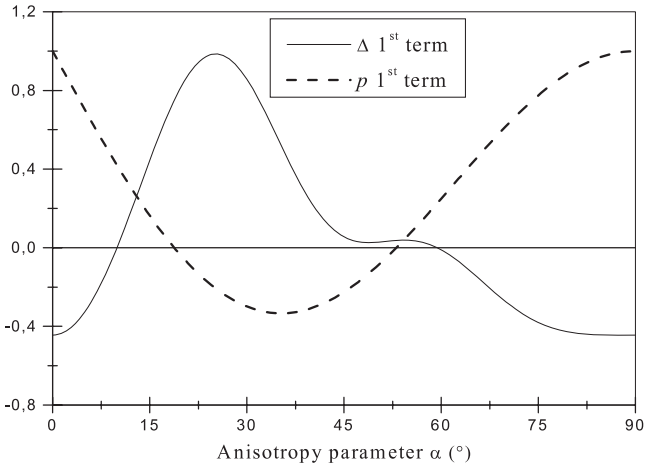

Figure 3. Δ and p signs as a function of the anisotropy parameter.

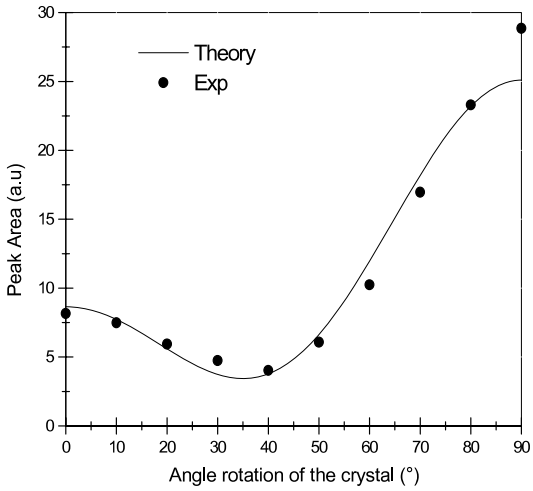

Figure 4. Peak area of the A_1 mode for parallel polarizers at 632 cm^{-1}.

3.8.2. Resolution of the third-order polynomial equation. With the change of variable,

$$\tan\theta = x - \frac{\cos\varphi_{dc}}{\tan\alpha} \tag{31}$$

the polynomial equation (30) becomes

$$x^3 - px - q = 0 \tag{32}$$

$$p = (1 - \sqrt{3}\cos\alpha\sin\varphi_{dc})(1 + \sqrt{3}\cos\alpha\sin\varphi_{dc})\frac{1}{\sin^2\alpha} \tag{33}$$

$$q = 2\sin^2\varphi_{dc}\cos\varphi_{dc}\frac{1}{\tan^3\alpha}. \tag{34}$$

The sign of Δ defined below indicates the number of real roots of equation (32):

$$\Delta = \left(-\frac{p}{3}\right)^3 + \left(\frac{q}{2}\right)^2. \tag{35}$$

The substitution of p and q by their respective expressions (33), (34) leads to

$$\Delta = -\left[\tfrac{1}{4}\cos^2\alpha\sin^2(2\alpha)\sin^4\varphi_{dc} - \frac{1}{3}\cos^2\alpha\sin^2\varphi_{dc} + \frac{1}{27}\right]\frac{1}{\sin^6\alpha}. \tag{36}$$

We have resolved equation (32) and we do not find another expression for the phase difference. This is a proof of its uniqueness. Therefore the expressions of the phase differences (20) we have obtained for perpendicular polarizers are unique solutions.

4. Applications and experimental results

For applications, we have to replace in all the above relations the phase difference by its positive value less than π, which is $\varphi_{dc} = \pi - 2\alpha$ obtained for a lithium niobate crystal. One of the extrema positions is $\pi/2$. The others depend on p and Δ signs. These signs depend on the value of the anisotropy parameter α. Their knowledge can give us a general view of the existence of all types of solutions. The number of real roots corresponds to the number of extrema positions that we are supposed to find during the experimental simulations. To display this maximum, experimental simulations should be done in intervals corresponding to the period of the theoretical function. Figure 3 displays p and Δ signs demonstrating the different roots of the polynomial equation as a function of the anisotropy parameter α.

Table 1 presents some results of the Raman line fitting for three angle values of the crystal rotation. The error is calculated using the combination of errors from ω_0, Γ and A_0. So we have used equations (4) and (5) to find errors on S.

Table 2 is a comparison of the optical phonon modes of the present work with those of Nippus [3] and Barker and Loudon [8]. In table 1, we can see that the full width at half-maximum changes with the crystal rotation angle. In these last two works, the crystal rotation effect on the Raman line parameters has not been studied. So we compared these previous results with ours, obtained at $\theta = 0°$. For some phonon frequencies, our results are close to those of Nippus [3] and, for some others, they are close to those of Barker and Loudon [8].

Using the complete results of area fitting, we have plotted the Raman efficiencies or peak areas for two modes. These areas have been normalized by that of the A_1 mode for 0° measured at 253 cm^{-1}. Figure 4 displays the evolution of the peak area (equation (23)) with the crystal rotation angle for the A_1 mode at 632 cm^{-1}. Figure 5 displays the evolution of the peak area (equation (26)) with the crystal rotation angle for the Ey mode at 369 cm^{-1}. Table 3 presents the phase differences, the anisotropy factors (A.Fac) and a comparison with [3] results.

5. Discussions and conclusion

We can see from these three tables that the results of Nippus [3] and the present work are very similar for A_1 and Ey modes. The slight difference observed can be due to the fact that Nippus has considered that the relative

Table 1. Peak areas.

Angle	ω_0 (cm^{-1})	A_0	Γ_0 (cm^{-1})	S_{max}	S^a	$N.S^b$	$E.S^c$ (%)
0°	154	5.7	13.5	124.2	137.5	0.56	10.3
	253	10.6	17	223.7	247.7	1.00	7.6
	276	14.6	19	290.1	321.2	1.30	6.6
	369	0.9	13.5	29.7	32.8	0.13	23.3
	433	2.3	12.6	91.9	101.7	0.41	14.2
	580	8.6	31.5	167.8	185.8	0.75	5.1
	633	63	23	1825.1	2020.3	8.16	4.8
50°	154	17.6	13.3	389.5	431.2	1.74	8.7
	253	69.3	24.5	1017.2	1126.1	4.55	4.7
	276	25.4	12.6	757.5	838.5	3.39	8.9
	369	3.8	20.3	82.2	91	0.37	9
	433	2	9.8	98.5	109	0.44	17.7
	579	11.4	21	335.4	371.3	1.50	6.3
	633	47.3	23.1	1358.3	1503.6	6.07	4.9
90°	253	259	18.2	5125.6	5674	22.91	5.9
	276	107.1	12.6	3197.9	3540.1	14.29	8.4
	633	47.3	17.5	6456.2	7147	28.85	6.1

[a] area; [b] normalized area; [c] error in area.

Table 2. Optical phonon modes in $LiNbO_3$ at 300 K.

E symmetry mode				A_1 symmetry mode			
ω_0 (cm^{-1})	Γ (cm^{-1}) [a]	Γ (cm^{-1}) [b]	Γ (cm^{-1}) [c]	ω_0 (cm^{-1})	Γ (cm^{-1}) [a]	Γ (cm^{-1}) [b]	Γ (cm^{-1}) [c]
154	13.5	12	17	253	17	26	28
369	13.5	22	20	276	19	12	20
433	12.6	12	17	633	23	24	28
580	31.5	26	29				

[a] present results; [b] reference [3] results; [c] reference [8] results.

Table 3. Phase differences and anisotropy factors.

Mode	ω_0 (cm^{-1})	β, α (deg) [a]	$\varphi_{ba}, \varphi_{dc}$ (deg) [b]	A.Fac [c]	$(A.Fac)^{-1}$	$(A.Fac)^{-1}$ [3]
A_1	253	75.4	150.8	3.84	0.26	0.29
	276	71.2	142.4	2.94	0.34	0.44
	633	59.6	119.2	1.70	0.59	0.64
E_2	154	78.4	23.2	2.44	0.41	0.37
	369	71.5	37	1.49	0.67	0.46
	432	58.2	63.6	0.81	1.24	0.73
	580	65.4	49.2	1.09	0.92	0.55

[a] Anisotropy parameter for A_1 and Ey modes, respectively.
[b] Phase difference for A_1 and Ey modes, respectively.
[c] Anisotropy factor.

integrated areas are exactly equal to the square of the relative Raman polarizabilities. This is not quite exact because the proportionality coefficient depends on the phonon frequency. Strach [4] has determined some expressions of the Raman efficiencies as a function of the polarizer directions, but he did not use an adapted mathematical approach to determine with better accuracy the relative Raman tensor elements.

In conclusion, the theoretical study of the Raman efficiencies shows that the anisotropy parameters α and β are useful for the direct determination of anisotropy factors. We have established direct relations between peak areas and Raman efficiencies. These expressions are more convenient for fitting. Moreover, knowledge of the Raman efficiency theoretical behaviour is important for the prediction of the experimental curve behaviour, even for the nonlinear case. Our method is adapted for this study because it also allows us to determine numerous crystal characteristics, namely the anisotropy parameters, anisotropy factors and phase differences. This method is systematic and leads to accurate results. It is a general method applicable to other C_{3v} crystals.

It would be more interesting to compare the phase differences and the anisotropy factors given in table 3 from the present work with those calculated from the quantum mechanical calculations based on atomic sphere approximation (ASA) linear muffin tin orbital (LMTO) band structures [9]. Such a comparison has been carried out by Strach [4] in the study of $S_mBa_2Cu_3O_{7-\delta}$ superconductors for different laser energies. As a consequence, the present work has to be extended to other laser lines in order to provide experimental datasets for further theoretical investigations.

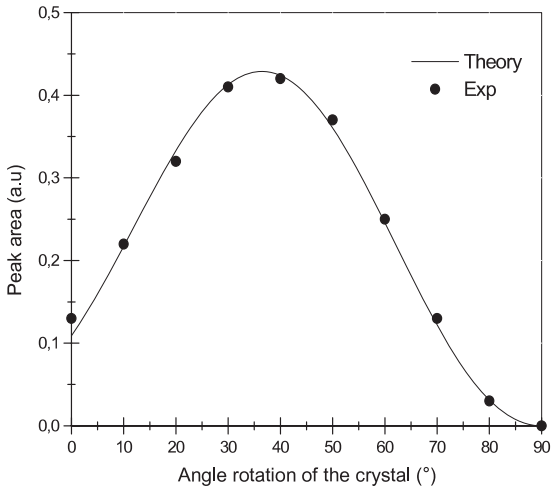

Figure 5. Peak area of the Ey mode for parallel polarizers at 369 cm^{-1}.

Acknowledgments

One of the authors (ND) would like to address special thanks to the ICTP for partially supporting him during the period of this work via the OEA-AC-71 project. Thanks are also addressed to the African Laser Centre (ALC) for its financial support. Special thanks are addressed to Dr R Erasmus for his careful reading of this paper.

Appendix A. Study of the Raman intensity $I_{yy}^{A1(\theta)}$

A.1. Linearization and period

Let

$$\cos\beta = \frac{|a|}{\sqrt{|a|^2+|b|^2}}, \qquad \sin\beta = \frac{|b|}{\sqrt{|a|^2+|b|^2}}. \tag{A.1}$$

The linearization of equation (8) leads to the following periodical equation with period $T = \pi$:

$$\begin{aligned} I_{yy}^{A_1(\theta)} &= |a|^2(1+(\tan\beta)^2)[\tfrac{3}{8}+\tfrac{1}{8}\sin(2\beta)\cos\varphi_{ba} \\ &+ \tfrac{1}{2}\cos(2\beta)\cos(2\theta) \\ &- (\sin(2\beta)\cos\varphi_{ba}-1)\cos(4\theta)]. \end{aligned} \tag{A.2}$$

A.2. Phase difference and extrema positions

The first derivative of (A.2) with respect to the angle θ is equal to zero under the conditions

$$-\cos 2\beta + (\sin 2\beta\cos\varphi_{ba}-1)\cos 2\theta = 0, \qquad \sin 2\theta = 0. \tag{A.3}$$

These conditions are respectively equivalent to

$$\cos\varphi_{ba} = \frac{\cos(2\theta_0)+\cos(2\beta)}{\cos(2\theta_0)\sin(2\beta)} \tag{A.4}$$

θ_0 being the position of an extremum:

$$\theta = \frac{2k\pi}{2}, \qquad \theta = \frac{\pi}{2}+\frac{2k\pi}{2} \qquad k\in\{0,1\}. \tag{A.5}$$

Equation (A.4) contains two unknown parameters (φ_{ba}, θ_0) depending on the parameter β.

So, the phase difference is unknown explicitly, the same as the extrema positions.

In the following, we have used a mathematical approach to separate these parameters.

A.2.1. Phase difference. Seeing that equation (A.4) contains $\cos(2\beta)$ and $\sin(2\beta)$, we rewrite it as

$$\left(\frac{\cos(2\theta_0)+\cos(2\beta)}{\cos(2\theta_0)\cos(2\beta)}\right)\cos(2\beta) - \sin(2\beta)\cos\varphi_{ba} = 0. \tag{A.6}$$

Let

$$\sin\varphi_{ba} = \pm\frac{\cos(2\theta_0)+\cos(2\beta)}{\cos(2\theta_0)\cos(2\beta)}. \tag{A.7}$$

Equation (A.6) becomes

$$\sin(\varphi_{ba}\pm 2\beta) = 0 \tag{A.8}$$

or

$$\tan(\varphi_{ba}) = \tan(\pm 2\beta) \tag{A.9}$$

(A.8) and (A.9) have naturally the same solutions given by

$$\varphi_{ba} = \pm 2\beta \tag{A.10}$$

or

$$\varphi_{ba} = \pm(\pi \pm 2\beta). \tag{A.11}$$

The sign + or − takes into account the fact that b is damped with respect to a or conversely.

It is found from the experimental data that the optimal solution of (A.6) is then expressed by (A.11).

A.2.2. Extrema positions. Consider the general equation

$$\sin^2\varphi + \cos^2\varphi = 1 \tag{A.12}$$

we substitute in this equation the expressions for $\sin\varphi_{ba}$ and $\cos\varphi_{ba}$. We obtain a second degree equation whose variable is $\cos(2\theta_0)$:

$$\begin{aligned} &(1-\sin^2(2\beta)\cos^2(2\beta))\cos^2(2\theta_0) + 2\cos(2\beta)\cos(2\theta_0) \\ &\quad + \cos^2(2\beta) = 0. \end{aligned} \tag{A.13}$$

Solving this equation, the two solutions are

$$\cos(2\theta_0) = \frac{\cos(2\beta)}{-1+\sin(2\beta)\cos(2\beta)} \tag{A.14}$$

or

$$\cos(2\theta_0) = \frac{\cos(2\beta)}{-1-\sin(2\beta)\cos(2\beta)}. \tag{A.15}$$

These solutions can also be obtained by using equation (A.4). Therefore, solution (A.14) is the one we can obtain with the phase difference (A.10) and solution (A.15) can be obtained with the phase difference (A.11). So, the optimal solution is (A.14) according to experimental measurements. Meanwhile, the sign of the phase difference is not determined. These two values of the phase differences lead to the same Raman scattering intensity because the cosine is an even function. The space range of the parameter can be known by using the restricting condition:

$$-1 \leqslant \cos(2\theta_0) \leqslant 1 \tag{A.16}$$

$$\beta \in]28,6^\circ; 90^\circ[. \tag{A.17}$$

A.3. Raman efficiency expression

Substituting the phase difference in the Raman expression (8) by its expression given by (A.10) and using (A.1), we can then rewrite the expression of the corresponding Raman intensity as

$$I_{yy}^{A_1(\theta)} = |a|^2(1 + (\tan\beta)^2)[\cos^2\beta\cos^4\theta + \sin^2\beta\sin^4\theta + \tfrac{1}{8}\sin(4\beta)\sin^2(2\theta)] \quad \text{(A.18)}$$

where we can see that the Raman intensity is now expressed as a function of only two parameters $|a|$ and β.

Appendix B. Study of the Raman intensity $I_{yz}^{Ey(\theta)}$

B.1. Linearization and period

Let

$$\cos\alpha = \frac{|c|}{\sqrt{|c|^2 + 4|d|^2}}, \qquad \sin\alpha = \frac{2|d|}{\sqrt{|c|^2 + 4|d|^2}}. \quad \text{(B.1)}$$

The linearization of (10) leads to the following periodical function with a period $T = \pi/2$:

$$I_{yz}^{Ey(\theta)} = \tfrac{1}{8}|c|^2(1 + (\tan\alpha)^2)[1 - \cos(2\alpha)\cos(4\theta) - \sin(2\alpha)\sin(4\theta)\cos(\varphi_{dc})]. \quad \text{(B.2)}$$

B.2. Phase difference and extrema positions

The first derivative of (B.2) with respect to the angle θ is equal to zero for the condition

$$\cos(2\alpha)\sin(4\theta_0) - \sin(2\alpha)\cos\varphi_{dc}\cos(4\theta_0) = 0. \quad \text{(B.3)}$$

Equation (B.3) has two unknown parameters which are the phase difference and the extrema position, respectively (φ_{dc}, θ_0) depending on the parameter α. So we have to separate these unknown parameters and express each of them as a function of α. With the aim of separating the variables, we rewrite (B.3) as follows:

$$\cos\varphi_{dc} = \frac{\tan(4\theta_0)}{\tan(2\alpha)}. \quad \text{(B.4)}$$

B.2.1. Phase difference. Equation (B.3) can also be rewritten as

$$\tan(4\theta_0)\cos(2\alpha) - \sin(2\alpha)\cos\varphi_{dc} = 0. \quad \text{(B.5)}$$

Let

$$\sin\varphi_{dc} = \pm\tan(4\theta_0). \quad \text{(B.6)}$$

Therefore, equation (B.5) becomes

$$\sin(\varphi_{dc} \pm 2\alpha) = 0 \quad \text{(B.7)}$$

or

$$\tan(\varphi_{dc}) = \tan(\pm 2\alpha). \quad \text{(B.8)}$$

Equations (B.7) and (B.8) have the same solutions which are given by

$$\varphi_{dc} = \pm 2\alpha \quad \text{(B.9)}$$

or

$$\varphi_{dc} = \pm(\pi \pm 2\alpha). \quad \text{(B.10)}$$

The sign + or − takes into account the fact that d is damped with respect to c or conversely.

According to the experimental results, the optimal solution is given by (B.10).

B.2.2. Extrema positions. Substituting in the general equation (A.12) the expressions for cosine and sine by their above values, we obtain a second degree equation. Its resolution yields

$$\tan(4\theta_0) = \sin(2\alpha) \quad \text{(B.11)}$$

or

$$\tan(4\theta_0) = -\sin(2\alpha). \quad \text{(B.12)}$$

Solving equations (B.11) and (B.12), the peak positions are given by

$$\theta_0 = \frac{k\pi}{4} + \arctan(\sin(2\alpha)) \quad \text{(B.13)}$$

or

$$\theta_0 = \frac{k\pi}{4} + \arctan(-\sin(2\alpha)) \qquad k \in \{0, 1, 2, 3\}. \quad \text{(B.14)}$$

Using the derived equation (B.5), solution (B.13) is the one we can obtain with the phase difference (B.9) and (B.14) can be obtained with the phase difference (B.10).

According to the experimental simulations, the optimal result is given by (B.14).

B.3. Raman efficiency

Now that the phase difference is expressed as a function of the parameter α we can rewrite the Raman efficiency in a useful form as follows:

$$I_{yz}^{Ey(\theta)} = \tfrac{1}{8}|c|^2(1 + \tan^2\alpha)[1 - \cos(2\alpha)\cos(4\theta) + \tfrac{1}{2}\sin(4\alpha)\sin(4\theta)]. \quad \text{(B.15)}$$

Comparing equations (10) and (B.15), we can see that the number of parameters has been reduced from 3 to 2. This is an important result that simplifies the fitting of the spectra.

References

[1] Mooradian A and McWhorter A L 1967 Polarization and intensity of Raman scattering from plasmons and phonons in gallium arsenic *Phys. Rev. Lett.* **19** 849

[2] Loa I, Gronemeyer S, Thomsen C, Ambacher O, Schikora D and As D J 1998 Comparative determination of absolute Raman scattering efficiencies and application to GaN *J. Raman Spectrosc.* **29** 291–5

[3] Nippus M 1976 Relative Raman-intensitäten der phononen von $LiNbO_3$ *Z. Naturf.* a **31** 231–5

[4] Strach T, Brunen J, Lederle B, Zegenhagen J and Cardona M 1998 Determination of the phase difference between the Raman tensor elements of the A_{1g}-like phonons in $S_mBa_2C_{u3}O_{7-\delta}$ *Phys. Rev.* B **57** 1292

[5] Djiedeu N, Mohamadou B, Bourson P and Aillerie M 2008 Determination of the Raman polarizabilities of optical phonons in lithium niobate uniaxial single crystal *Ann. Phys. (EDP Sciences)* at press

[6] Penna A F, Chaves A, Andrade P da R and Porto S P S 1976 Light scattering by lithium tantalate at room temperature *Phys. Rev.* B **13** 4907
[7] Barker A S Jr and Loudon R 1972 Response functions in the theory of Raman scattering by vibrational and polariton mode in dielectric crystals *Rev. Mod. Phys.* **44** 18
[8] Barker A S Jr and Loudon R 1967 Dielectric properties and optical phonons in $LiNbO_3$ *Phys. Rev.* **158** 433
[9] Heyden E T, Rashkeev S N, Mazin I I, Andersen O K, Liu R, Cardona M and Jepsen O 1990 Resonant Raman scattering in $YBa_2Cu_3O_7$: band theory and experiment *Phys. Rev. Lett.* **65** 3048